Journal of Building Pathology and Rehabilitation (2023) 8:93
https://doi.org/10.1007/s41024-023-00340-z

RESEARCH ARTICLE

Investigating the behavior of composite steel–concrete beams with X-HVB shear connectors exposed to various fire temperature levels

Mays A. Hamad[1,2] · **Haitham H. Muteb**[1] · **Mustafa S. Salah**[3]

Received: 17 July 2023 / Revised: 11 August 2023 / Accepted: 13 August 2023 / Published online: 19 August 2023

Abstract
Composite steel–concrete beams are widely used in modern construction due to their advantageous structural behavior and efficiency. The performance of these beams under fire is crucial for ensuring their fire resistance and structural integrity. This paper investigates the performance of composite steel–concrete beams with X-HVB shear connectors after exposure to different levels of temperature, considering the effect of the direction of the profiled steel plate to the steel beam length. Experimental work was conducted using eight composite beam specimens to assess their load carrying capacity, stiffness, ductility and energy absorption under varying temperature degrees and corrugated steel plate orientations (parallel or transverse to the beam length). The results indicate that the load carrying capacity, stiffness, and ductility of the composite beam specimens decrease with increasing exposure temperature level. Furthermore, the orientation of the profiled steel plate was found to significantly influence the beam's performance. By examining different temperature levels and the influence of corrugated steel plate orientation, valuable insights are gained regarding the fire resistance and structural performance of these beams. These insights can inform the design and implementation of composite structures, ensuring their safety and durability in fire-prone environments.

Keywords Composite steel—concrete beam · X-HVB · Fire · Composite action · Profiled steel plate

1 Introduction

Composite steel–concrete beams are widely utilized in modern construction due to their favorable structural performance and efficiency. These beams typically consist of a steel section acting compositely with a reinforced concrete decks, resulting in a lightweight and durable structural system. A solid reinforced concrete slab, a precast hollow core slab, or a composite slab with Profiled Steel Plate (PSP) are all options for reinforced concrete decks. Shear connectors are key components to ensure efficient composite action and satisfactory transfer of shear forces at composite beams steel–concrete interface. However, the behavior and performance of composite beams can be significantly affected when exposed to elevated temperatures during fire incidents [1, 2].

In recent years, a new shear connector type adopted by Hilti company and denoted by the symbols X-HVB has emerged as a promising alternative for enhancing the shear connection in composite steel–concrete beams. The X-HVB connectors are specifically designed to resist shear forces and sustain the structural integrity of the composite system. Studies have shown that the behavior of X-HVB connectors is ductile and comparable to that of stud shear connectors [3]. However, the behavior of composite steel–concrete beams with X-HVB shear connectors under fire conditions is an area that requires thorough investigation. Fire

✉ Mays A. Hamad
mays.abdal_redha@uomus.edu.iq;
mays.hamad.engh345@student.uobabylon.edu.iq

Haitham H. Muteb
eng.haitham.hassan@uobabylon.edu.iq

Mustafa S. Salah
mustafa.sa@uowa.edu.iq

1 College of Engineering, University of Babylon (UoB), PO box 247, Hilla, Iraq

2 Building and Construction Techniques Engineering Department, Al-Mustaqbal University, Hillah, Babil 51001, Iraq

3 Civil Engineering Department, College of Engineering, University of Warith Al-Anbiyaa, Karbala 56001, Iraq

incidents pose significant challenges to structural systems, as elevated temperatures can lead to material degradation, loss of strength, and potential failure [4]. To ensure fire resistance and structural stability of composite beams, it is crucial to comprehend the behavior of composite steel—concrete beams with X-HVB shear connectors exposed to different levels of fire temperatures.

Building upon the previous research efforts, several studies have examined different aspects of the fire resistance of composite beams and floor systems. Lyu et al. [5] investigated the fire resistance of composite beams with restrained superposed slabs. They found that the temperature of the concrete superposed slabs decreased along their heights, with the lowest temperatures near the bottom. They also found that the spacing of shear studs in the composite beams had a significant impact on their fire resistance. Kodur et al. [6] developed a 3D nonlinear finite element model to evaluate composite beam–slab assemblies under gravity and fire loading. The model considered different shear connection types and fire scenarios. It accounted for temperature-dependent properties and validated the accuracy by comparing predicted and measured responses of tested assemblies. The research highlights the significant improvement in fire performance due to composite action.

Jian-chun et al. [7] conducted two full-scale tests on steel–concrete composite beams to study their catenary action under fire. They found that the changing temperature distribution generated additional bending moments, negatively affecting the ultimate bearing capacity of the composite beam. They also found that load ratio was a crucial parameter affecting the fire resistance of the composite beam, with larger load values resulting in more pronounced catenary action under the same conditions. Kodur and Naser [8] proposed a new approach for evaluating the degradation of shear capacity of composite beams under fire by considering the effect of temperature-induced strength loss and sectional instability in web. Ding et al. [9] conducted numerical simulations on stainless steel–concrete composite beams to assess their fire resistance. They found that the stainless steel's thermal expansion had a significant impact on the fire resistance of these composite beams. They proposed a simplified method for temperature distribution and introduced a coefficient for temperature-induced bending moment, improving the accuracy of fire-resistant design for these composite beams.

Li and Zhou [10] carried out fire tests on two simply supported composite beams made of ordinary structural steel. They found that the mechanical properties and failure modes of the composite beams with different direction of sheeting rib under fire were significantly different. They also proposed a simplified calculation method for the temperature field distribution and mechanical model of composite beams under fire. Wang et al. [11] investigated the fire behavior of steel–concrete composite beams (SCB) and partially encased steel–concrete composite beams (PEB) through numerical analysis and validated their models with experiments. They found that both types of beams experienced four deformation stages under fire. They also found that PEB required additional measures and fire protection layers to achieve class I fire resistance, while SCB needed at least 15 mm of fire protection. They introduced a coefficient related to fire time to modify the ultimate flexural capacity formula for SCB and PEB, resulting in accurate predictions. Choi [12] studied headed shear studs in transverse trapezoidal decks and solid slabs under ambient and fire conditions. They found that failure in solid slabs was concrete-dominated, but in transverse decks, it transitioned to stud shearing at higher temperatures. They also found that Eurocode guidance was conservative for transverse decks, and proposed a new design formula for shear connection capacity. Rodrigues and Laím [13] examined the structural behavior of T, T-block, and T-Perfobond shear connectors under fire conditions. They found that the shape of the connectors relative to the steel beam significantly affected their shear resistance capacity at elevated temperatures. They emphasized the importance of considering connector shape in fire-resistant design.

While other studies, such as those conducted by Fike and Kodur and Wang et al., have explored various aspects of enhancing the fire resistance of composite beams. Fike and Kodur [14] highlighted the effectiveness of using steel fiber reinforced concrete to enhance the fire resistance of composite floor assemblies. Their research demonstrated the improved strength, crack resistance, and spalling resistance of concrete when steel fibers are incorporated. Wang et al. [15] investigated the behavior of composite beams under fire exposure and examined the effect of shear connection ratio on their performance. They concluded that shear connection ratio had minimal influence on fire performance time, suggesting that alternative shear connectors could be explored to improve fire resistance. In a similar vein, Nguyen and Park [16] explored the impact of insulation materials and loading conditions on the fire resistance of composite I-beams. Their research demonstrated that the presence of insulation materials contributed to delaying failure time and reducing deformation, thereby enhancing the fire resistance of the beams. These findings offer valuable information for the design of fire-resistant structures.

However, further investigation is needed to understand the specific behavior of composite steel–concrete beams with the novel X-HVB shear connector under fire conditions. Therefore, this study aims to investigate the behavior of composite steel–concrete beams with X-HVB shear connectors when subjected to different fire temperature levels. The primary objective is to comprehensively analyze the behavior and failure modes of these innovative shear connectors under fire conditions and assess the overall structural response of the composite beams. By examining the performance of the X-HVB shear connectors in a fire environment, engineers and researchers can gain valuable insights into their fire resistance capabilities and develop effective strategies to enhance the fire safety of composite steel–concrete beams.

2 Hilti X-HVB shear connector

The X-HVB shear connector is a type of mechanical connector used to provide a shear connection between a steel beam and a concrete slab in composite steel and concrete structures [17]. The connector adopted by Hilti Corporation is more user-friendly than conventional types, and it is named after its shape, which resembles the letter X. Additionally, they have another variant called HVB, which stands for Headed and Bent Vertical [18]. The X-HVB shear connector is designed and tested in accordance with various international standards and codes, such as the American Institute of Steel Construction (AISC) [19] and the European Standard EN 1994-1-1 [20]. These standards provide guidelines for the design, fabrication, and installation of the connectors, ensuring that they meet the required performance criteria and are safe and reliable. The use of standard connectors also helps to facilitate the construction process, reducing the need for custom-designed connectors and simplifying the fabrication and installation process [18].

Hilti HVB shear connectors are cold formed angle shear connectors, fixed by two powder-actuated fasteners (XENP-21 HVB) driven with a powder-actuated tool (Hilti DX 76 or DX 76 PTR), placed on one leg of the angle, all these parts are shown in Fig. 1. It is possible to use one, two or three connectors in each steel decking rib, depending on the requirements [17]

The shear resistance of this type of connector is influenced by several factors, including hole elongation in the fastening leg, anchorage mechanism failure, bending of the fasteners, and deformation of the concrete in the connector's surrounding zone. In addition, even at low degrees of partial shear connection (20 percent), the X-HVB connector's behavior remains ductile, and its deflection does not exceed 1/300 of the span, with minimal loss of stiffness at the serviceability limit condition. Proper positioning of the connections allows the same formula used for shear studs to estimate the reduction in strength of the non-welded connectors due to the presence of profiled sheeting [21].

Table 1 Details of composite beam specimens

No	Specimen designation	The orientation of the profiled steel plate with respect to the beam span	Temperature (℃)
1	CDp	Parallel	35
2	$CDpT_{350}$	Parallel	350
3	$CDpT_{450}$	Parallel	450
4	$CDpT_{550}$	Parallel	550
5	CDt	Transverse	35
6	$CDtT_{350}$	Transverse	350
7	$CDtT_{450}$	Transverse	450
8	$CDtT_{550}$	Transverse	550

3 Experimental work

An experiment was conducted to investigate the behavior of X-HVB shear connectors in composite construction. The objective was to determine the capacity and load-slip behavior of the connectors under varying conditions, including exposure to fire at different temperatures (350 ℃, 450 ℃, and 550 ℃) and the orientation of the profiled steel plate (parallel or transverse to the beam's length). Eight composite beam specimens were tested, comprising a 0.9 mm thick profiled steel plate attached to

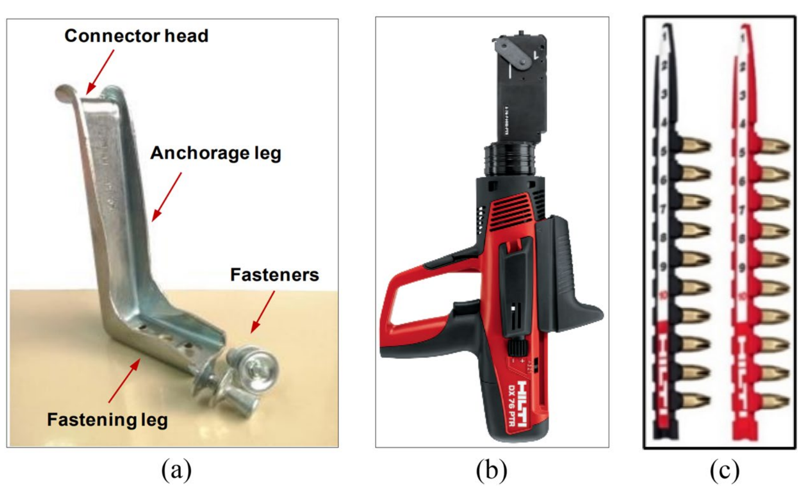

Fig. 1 Hilti X-HVB system. **a** X-HVB shear connector configuration with Two X-ENP-21 HVB Nails [22]. **b** DX 76 PTR tool [21]. **c** cartridges [21]

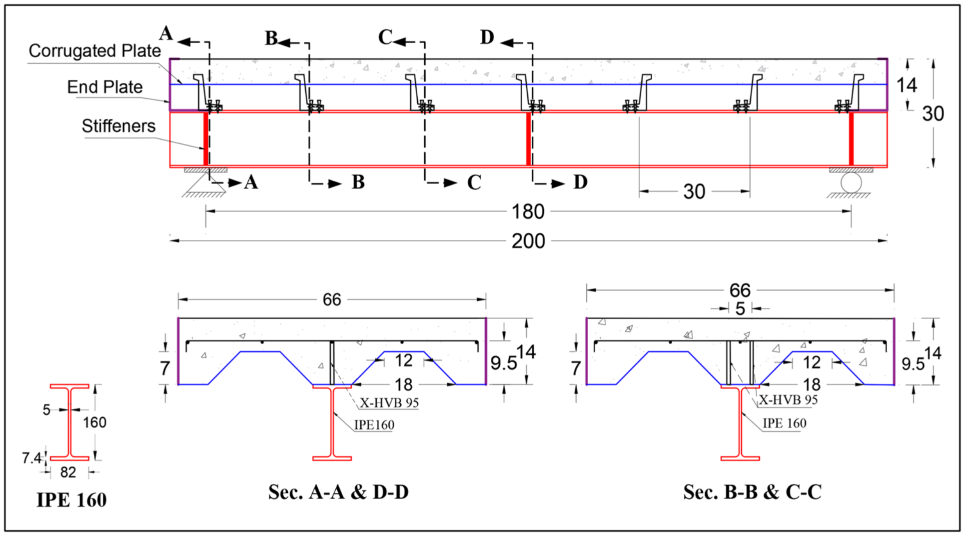

Fig. 2 Details of composite beam specimens with parallel profiled steel plate (dimensions in cm)

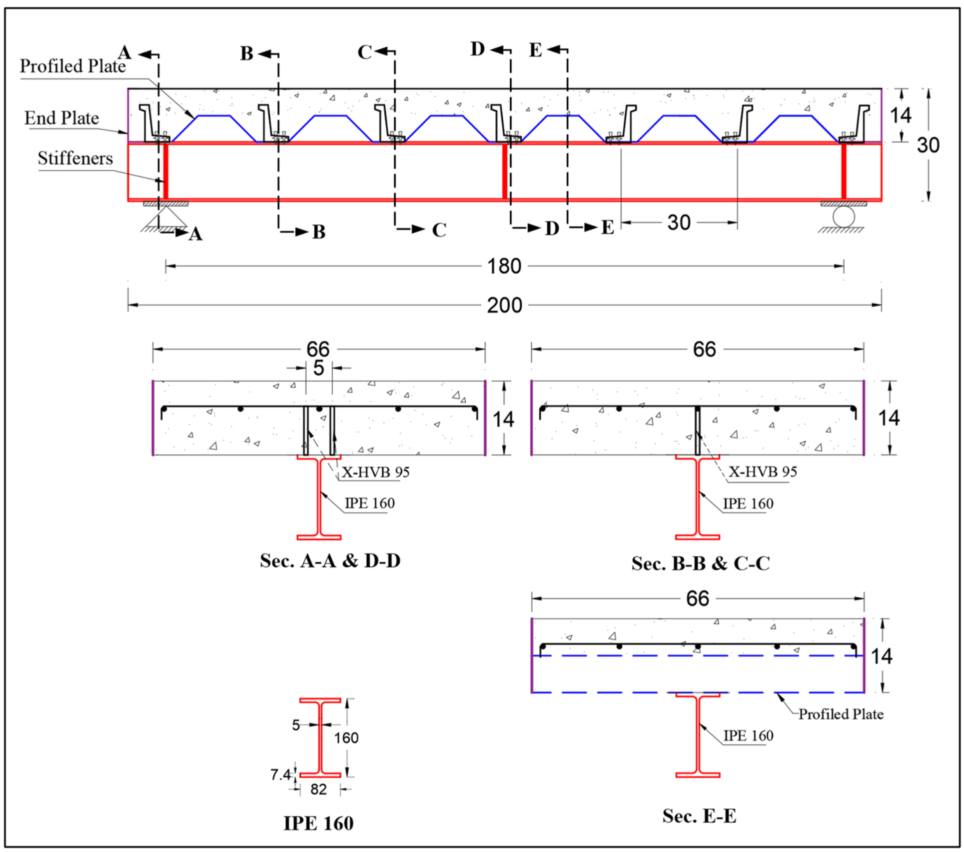

Fig. 3 Details of composite beam specimens with transverse profiled steel plate (dimensions in cm)

an IPE160 steel beam using X-HVB 95 shear connectors. Two specimens were tested at ambient temperature, while the others were exposed to fire prior to testing. Table1 provides detailed information about all the specimens used in the study, while Figs. 2 and 3 present a typical cross sections for the test samples. These specimens were prepared by cutting the profiled plate and steel beam to the required dimensions, fixing the shear connectors with a Hilti DX 76 machine, as shown in Fig. 4. Normal concrete with a strength of 37 MPa was used for concreting the specimens. To assess the compressive strength, twelve cubes measuring 150 × 150 × 150 mm were cast and subsequently curing. Among these cubes, three were subjected to testing under ambient temperature conditions, while the remaining underwent testing after being exposed to fire flames at varying temperature levels 350 ℃, 450 ℃, and 550 ℃.

Fig. 4 The fabrication steps for composite beam specimens: **a** preparation of profiled steel plate, **b** ipe160 steel section preparation, **c** x-hvb shear connector positioning, **d** mold preparation for casting, **e** concreting **f** curing of cast specimens

Fig. 5 The specimen nomination system

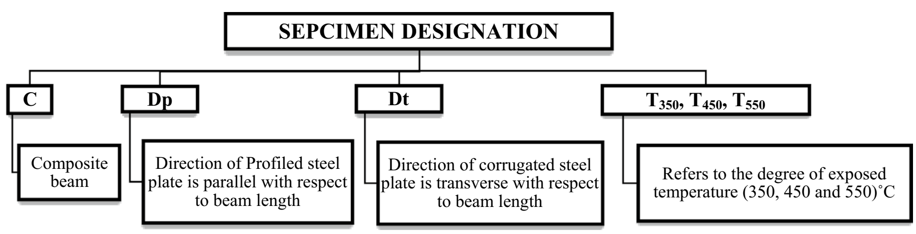

A nomination system was used to identify each specimen as depicted in Fig. 5. The specimens were denoted by the letter 'C' followed by the direction of the corrugated plate to the steel beam (parallel 'Dp' or transversely 'Dt'), and the temperature level to which it was exposed (T_{350}, T_{450}, or T_{550}), respectively.

3.1 Fire exposure process and furnace design

The fire exposure process took place in a specially manufactured furnace designed for burning structural members. The furnace has outer dimensions of 2200 × 1000 × 1250 mm (length × width × height) with 200 mm thick walls made of lightweight Thermostone brick and glue. Thermostone brick offers lightweight thermal insulation properties and can resist fire for up to 7 h. The furnace floor, also made of Thermostone, is 100 mm thick to provide complete thermal insulation from the bottom and prevent heat leakage. Additionally, small openings were drilled on two opposite sides of the furnace to ensure sufficient air supply for the burners. Figures 6 and 7 illustrate the details of the burning process and the furnace connections.

The burner network comprises six methane burners arranged in a single line on one side of the furnace, distributed along its length. These burners are connected through a pipeline to regulate the gas discharge. The main objective of the stove compartment is to raise the temperature levels of the fire exposure to the desired target temperature and then maintain the temperature constant for the required duration, following the ISO 834 standard fire curve. The fire exposure lasts for 60 min, with maximum temperature levels of 350 °C, 450 °C, and 550 °C maintained for each respective case, as depicted in Fig. 8. Additionally, the figure illustrates the correlation between the two temperature measurement methods: the digital thermocouple gauge and the newly incorporated infrared thermometer,

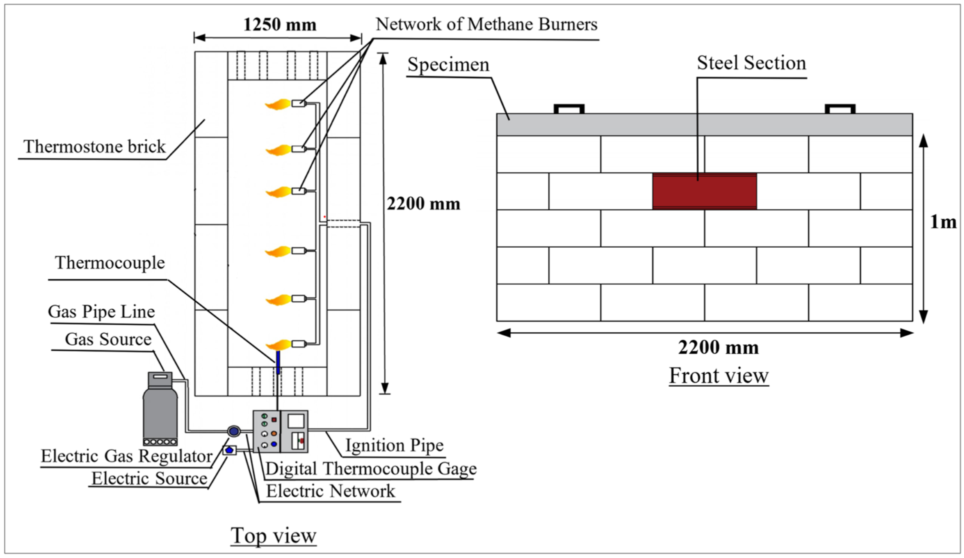

Fig. 6 Top and front view of the furnace and equipment

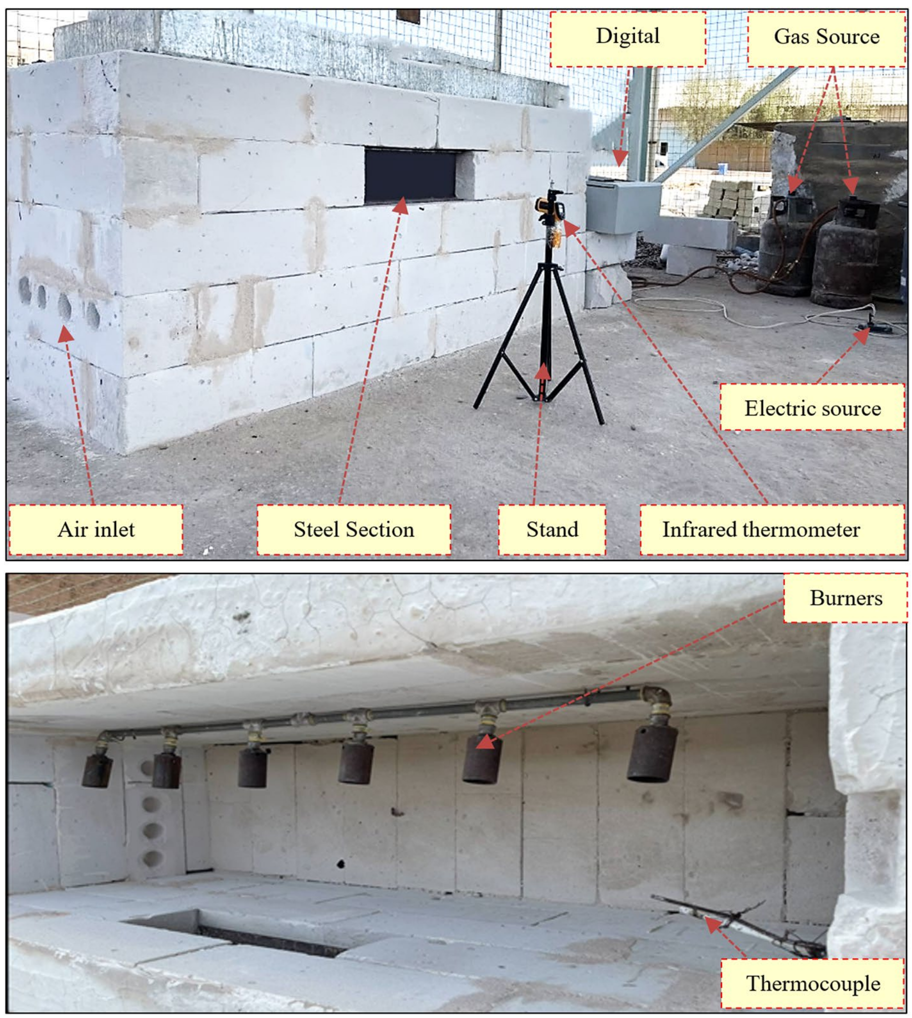

Fig. 7 The comprehensive description of the burning process and stove setup with connections

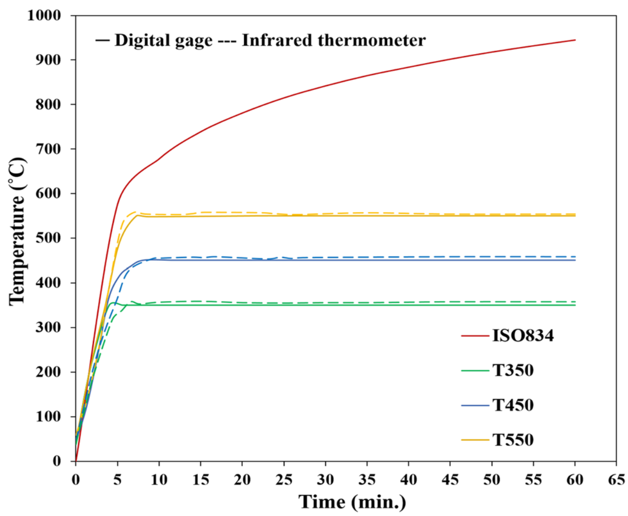

Fig. 8 Temperature evolution in the furnace

within the furnace. After the burning process is completed, the specimens are left in the stove compartment to cool down to ambient temperature before testing.

To regulate the burning procedure, a digital thermocouple gauge is used, as shown in Fig. 9a. The electric gas regulator and thermocouples are connected to the digital gauge, enabling control of the gas discharge and maintenance of the firing temperature at the predetermined target level set in the gauge before initiating the burning process. To ensure precise temperature measurement, a supplementary method was implemented using an infrared thermometer. The infrared thermometer is positioned at a fixed distance from the furnace to accurately monitor the temperature of the steel section. To replicate the air temperature inside the furnace, a modification was made by replacing the middle Thermostone brick on one side with the steel section, as depicted in Fig. 9b. This novel method was introduced to enhance temperature measurement accuracy.

3.2 Instrumentation and test procedures

The specimens were exposed to fire at three different temperature levels: 350 °C, 450 °C, and 550 °C, for a duration of 1 h. Afterward, they were gradually cooled to ambient temperature before undergoing testing. Additionally, two specimens were tested at ambient temperature. Figure 10 illustrates the instrumentation and setup of the specimens. The composite beam specimen is positioned on a rigid steel girder and supported by roller and hinge boundary conditions.

The testing procedure involved the utilization of two Linear Variable Differential Transformers (LVDTs). One LVDT was strategically positioned at the midpoint of the span from the bottom to measure displacement, while the other LVDT was placed at the side of the composite slab to measure slippage between the steel beam and the composite slab. To apply the load, a hydraulic jack with a capacity of 500 kN was employed, focusing on the mid-span of the composite beam. Additionally, a load cell (Data Logger) with a capacity of 300 kN was utilized to accurately measure the load.

To prevent local yielding in the steel and local crushing in the concrete, bearing plates were implemented at the supports and at the loading line, respectively. The load was gradually applied while continuously recording the self-weight and the initial deflection reading.

(a)

(b)

Fig. 9 Temperature measurement methods utilized in this study: **a** digital thermocouple gage, **b** infrared thermometer

Fig. 10 Description of the testing machine utilized in this study

4 Results and discussion

The results of the tests include the load-carrying capacity, load versus mid-span deflection, load versus slip between composite slab and steel beam, crack patterns, stiffness, ductility ratio, and energy absorption. All girders were tested under the same type of loading. Table 2 provides the results of the tested composite beams.

4.1 Load–defection response

Figure 11 illustrates the flexural response of the tested specimens with parallel profiled sheeting, whereas Fig. 12 illustrates the flexural response of the specimens with transverse profiled sheeting. The progression of mid-span vertical deflection is plotted against the applied load, comparing the effect of exposing the specimens to fire at temperatures of 350 °C, 450 °C, and 550 °C to the specimens tested at ambient temperature. The experimental results indicated that as the fire temperature level increased, there was a reduction in the load carrying capacity. At 350 °C, the specimens with profiled sheeting runs parallel to the steel beam experienced a loss of approximately 20%, while the specimens with profiled sheeting runs transversely lost about 23% compared to the corresponding specimens after 1-h fire exposure. At 450 °C, the loss increased to about 29% for specimens with parallel profiled sheeting and 33% for specimens with transverse profiled sheeting. Furthermore, at 550 °C, the loss further increased to about 36% for specimens with parallel profiled sheeting and 40% for specimens with transverse profiled sheeting compared to the corresponding specimens after 1-h fire exposure.

The observed decrease in the ultimate load capacity of the specimens exposed to fire primarily stems from the lower fire resistance of steel structures. This is mainly due to the high low specific heat and thermal conductivity of steel, leading to rapid temperature rise when subjected to fire. Moreover, the mechanical properties of steel, including strength and modulus, deteriorate more rapidly at elevated temperatures. Thus, the combined effect of these factors results in a reduction in the ultimate load capacity under fire exposure conditions.

Notably, when exposed to fire temperatures of 450 °C and 550 °C, all specimens exhibited sudden failure at smaller deflections, indicating shear connector failure. However, at ambient temperatures, failure occurred due to the yielding of the steel beam, resulting in failure at higher deflections.

Table 2 Summary of composite beam test results

Specimen	Ultimate load (kN)	Mid-span deflection (mm)	Peak slip (mm)	Ductility ratio	Stiffness (kN/mm)	Energy absorption(kN/mm)
CDp	219.86	34.39	6.18	3.46	16.59	5960.30
$CDpT_{350}$	176.74	20.80	2.81	2.27	14.44	2587.75
$CDpT_{450}$	155.56	12.98	2.13	1.56	14.06	1182.44
$CDpT_{550}$	140.17	11.77	1.72	1.46	13.03	895.01
CDt	190.98	32.73	6.60	4.94	21.64	5255.17
$CDtT_{350}$	147.56	12.56	2.52	1.69	14.90	693.52
$CDtT_{450}$	127.24	11.22	1.81	1.50	13.10	491.56
$CDtT_{550}$	114.00	10.15	1.57	1.41	12.44	616.08

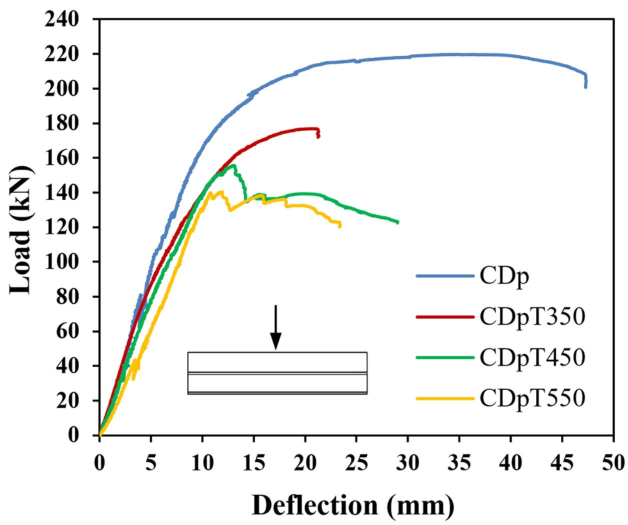

Fig. 11 Load versus deflection curve at mid-span of composite beam with parallel profiled sheeting

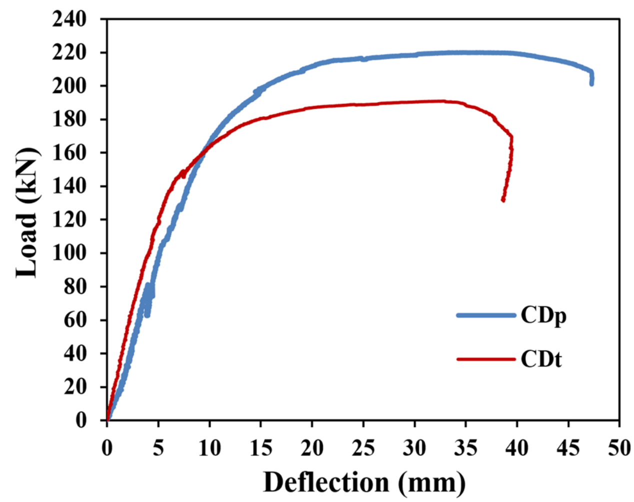

Fig. 13 Impact of profiled steel plate orientation on load–deflection curve at ambient temperature

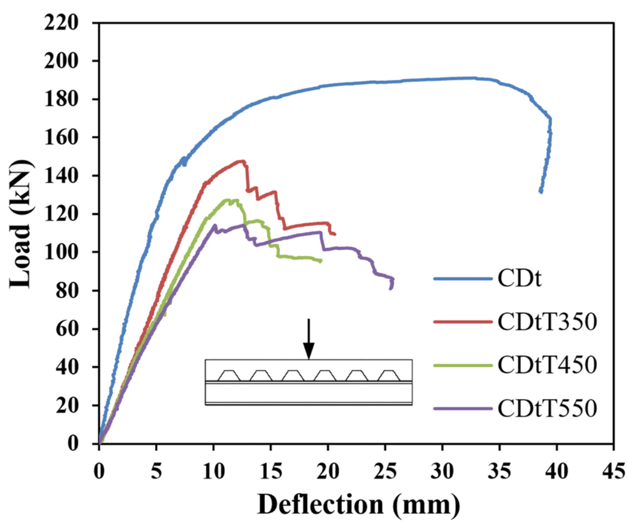

Fig. 12 Load versus deflection curve at mid-span of composite beam with transverse profiled sheeting

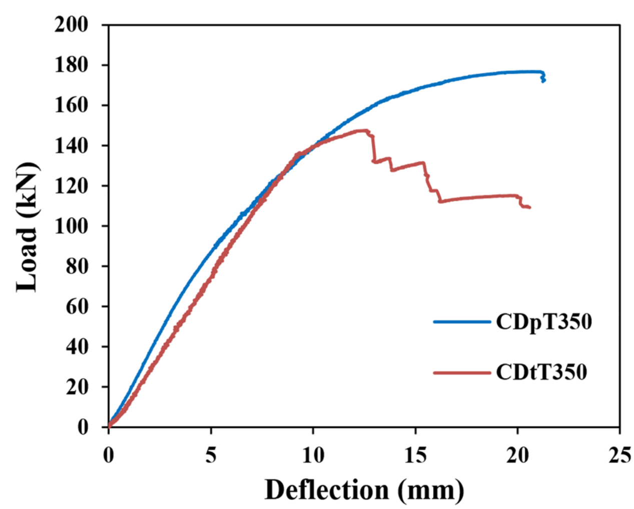

Fig. 14 Impact of profiled steel plate orientation on load–deflection curve at 350 ℃

Additionally, the ultimate deflection corresponding to the failure load decreased as the fire temperature increased. At 350 °C, the ultimate deflection reduced by approximately 62% and 40% for specimens with transverse and parallel profiled sheeting, respectively, compared to the corresponding control specimens. At 450 °C, the ultimate deflection decreased by around 62% and 66% for specimens with parallel and transverse profiled sheeting, respectively. Finally, at 550 °C, the ultimate deflection decreased by approximately 65% and 69% for specimens with parallel and transverse profiled sheeting, respectively, compared to the corresponding specimens.

Additionally, it is important to mention that all specimens with parallel profiled plate exhibited higher ultimate load compared to those with transverse profiled plate, as shown in Figs. 13, 14, 15, 16. However, the stiffness of the latter was higher. This is can be attributed to the different load distribution and deformation characteristics of the two configurations. Parallel profiled plates provide a more efficient load transfer mechanism between the steel beam and the concrete slab due to their alignment with the primary load paths. This alignment allows for better force distribution and load sharing, resulting in enhanced load-carrying capacity and ultimate strength.

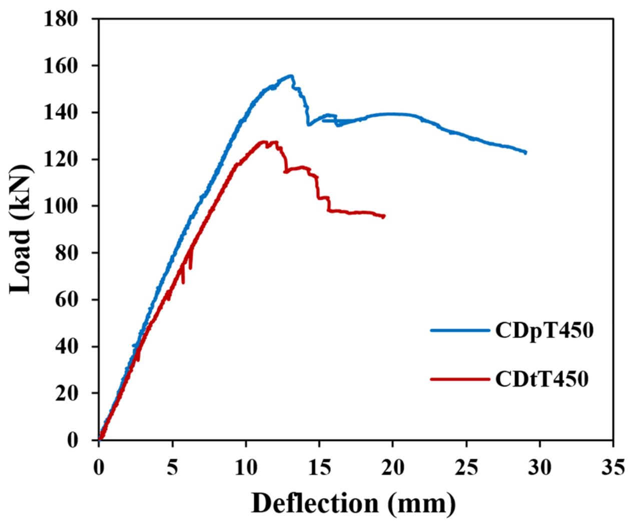

Fig. 15 Impact of profiled steel plate orientation on load–deflection curve at 450 ℃

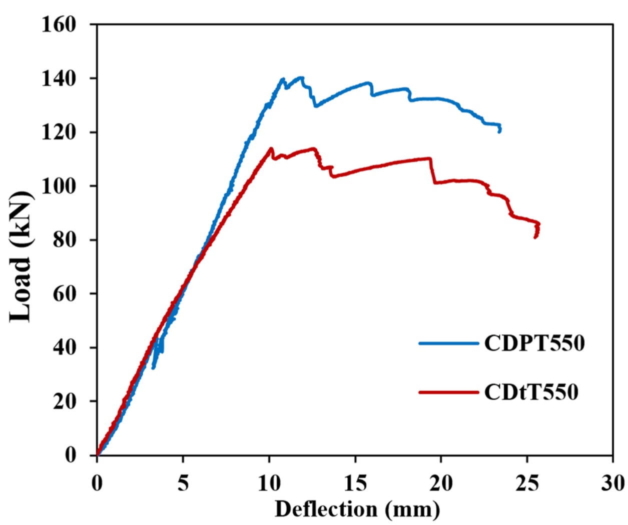

Fig. 16 Impact of profiled steel plate orientation on load–deflection curve at 550 ℃

On the other hand, transverse profiled plates may exhibit higher stiffness due to the orientation of the corrugations, which can resist deformation and flexural bending more effectively. This higher stiffness can contribute to reduced deflections and increased rigidity of the composite beam system. However, stiffness alone does not directly correlate with ultimate load capacity. The ultimate load capacity of a composite beam is influenced by factors such as load distribution, load-sharing mechanisms, and the ability to mobilize the full capacity of the materials involved. In the case of composite beam specimens with parallel profiled plates, the optimized load transfer efficiency and improved load-sharing characteristics contribute to a higher ultimate load capacity, despite potentially lower stiffness. The parallel orientation allows for better force transmission, reducing stress concentrations and enhancing the overall structural performance.

4.2 Load-slip response

The load-slip response of a composite beam connected with X-HVB shear connectors refers to the behavior of the beam in terms of applied load and the corresponding slip or displacement at the interface between the steel beam and the concrete slab. In the initial loading phase, the relative slips of the composite beam specimens were remained minimal owing to the strong interfacial bonding between the steel beam and the concrete slab, facilitated by the shear connector. However, as the applied load approached approximately 25% of the ultimate load, the slips escalated rapidly as a result of bond failure at the interface between the steel beam and the composite slab.

The load-slip response of composite beam specimens is affected by both the level of fire temperature and the orientation of the profiled sheeting with respect to the steel beam when subjected to fire exposure. For specimens with parallel profiled plate that exposed to temperature (350, 450 and 550 ℃) from steel section, the composite beam-end slip at ultimate load decreased by 54%, 65% and 72% than that of the unheated composite beam, respectively. While the reduction in specimen with transverse profiled plate by about 62%, 73% and 76% than that of the unheated composite beam as shown in Figs. 17 and 18. It was concluded that as the temperature increases, the ultimate relative slip of the composite beam specimen decreases. This is primarily due to the thermal effects on the materials involved. At higher temperatures, the structural components experience

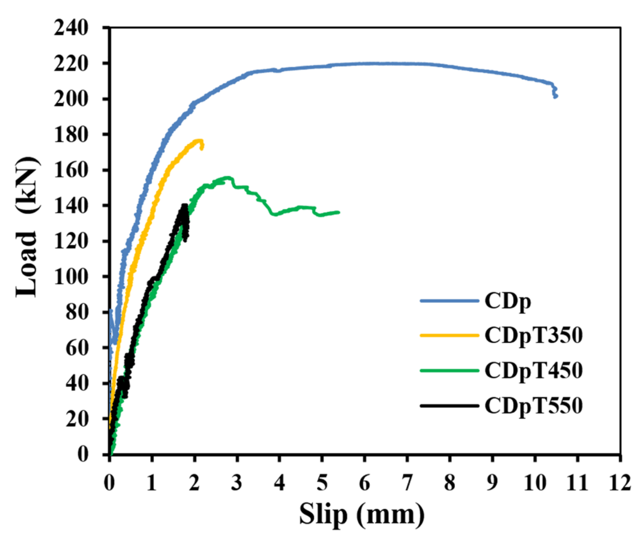

Fig. 17 Influence of exposure to fire on the shear resistance of X-HVB shear connectors with parallel profiled plate to the steel beam

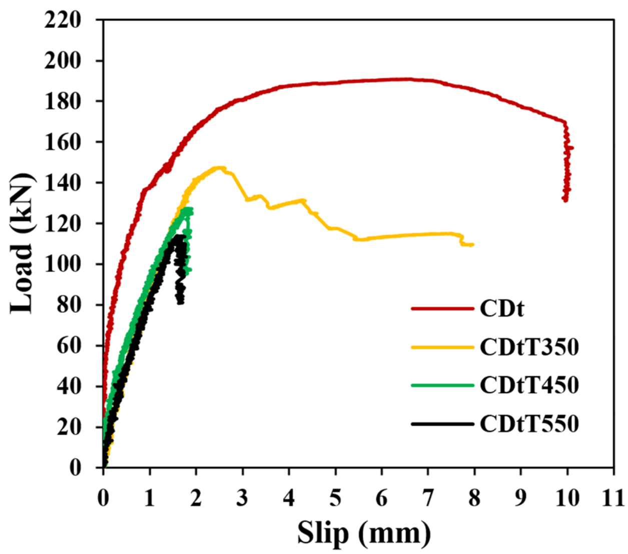

Fig. 18 Influence of exposure to fire on the shear resistance of X-HVB shear connectors with transverse profiled plate to the steel beam

thermal expansion and softening, resulting in reduced relative slip between the elements and a decrease in the overall load-bearing capacity.

It is also worth noting that the percentage decrease in ultimate slip is higher for specimens with transverse profiled sheeting compared to those with parallel profiled sheeting. This can be attributed to the difference in the orientation and arrangement of the profiled sheeting. The transverse profiled sheeting provides less resistance to slip due to its configuration, resulting in a larger decrease in ultimate slip compared to the parallel profiled sheeting. Additionally, the transverse orientation may affect the load transfer mechanism and contribute to a greater reduction in the ultimate slip of the composite beam specimen.

4.3 Failure mode

During the loading stage, visual observations were conducted to assess the behavior of both unburned and burned composite beam specimens exposed to different levels of firing. These observations aimed to capture the state of the specimens and study the development of failure mechanisms. As the specimens were exposed to fire, transverse cracks appeared at the top of the slab due to the thermal effects generated. These cracks were a direct consequence of the elevated temperatures experienced during fire exposure. Notably, approximately 16 min. after the initiation of the burning process, the cracks became permeable, allowing water and steam to seep through. This occurrence can be observed in Fig. 19, where the thermal cracks were clearly marked using a red marking pen.

The observations from the tests conducted on the specimens (CDp and CDt) showed that the dominant response and failure mode were related to flexural behavior. These specimens experienced significant degradation in flexural capacity, ultimately leading to failure through yielding of the steel beam.

In specimen CDp, a sudden appearance of longitudinal cracks was observed from the mid-span of the top face of the concrete slab to the support, with a width of 0.45 mm at a load of 80 kN. These cracks progressively propagated and widened until reaching the failure load. A blue marking pen was used to mark this crack. When subjected to a load of 126 kN, the shear connectors in the specimens became dislocated, resulting in a separation between the steel beam and the profiled slab. Furthermore, at a load of 206 kN, the top rib of the profiled steel plate exhibited buckling, occurring approximately 10 cm away from the load point. This behavior is illustrated in Fig. 20. Additionally, local buckling was observed in the steel beam under the applied load.

Fig. 19 Formation of transverse cracks due to the effects of fire during the fire process

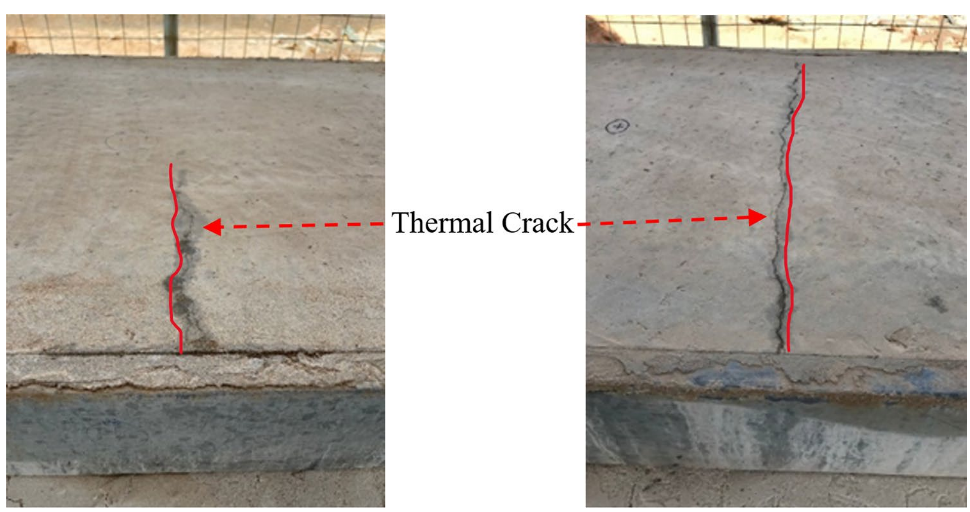

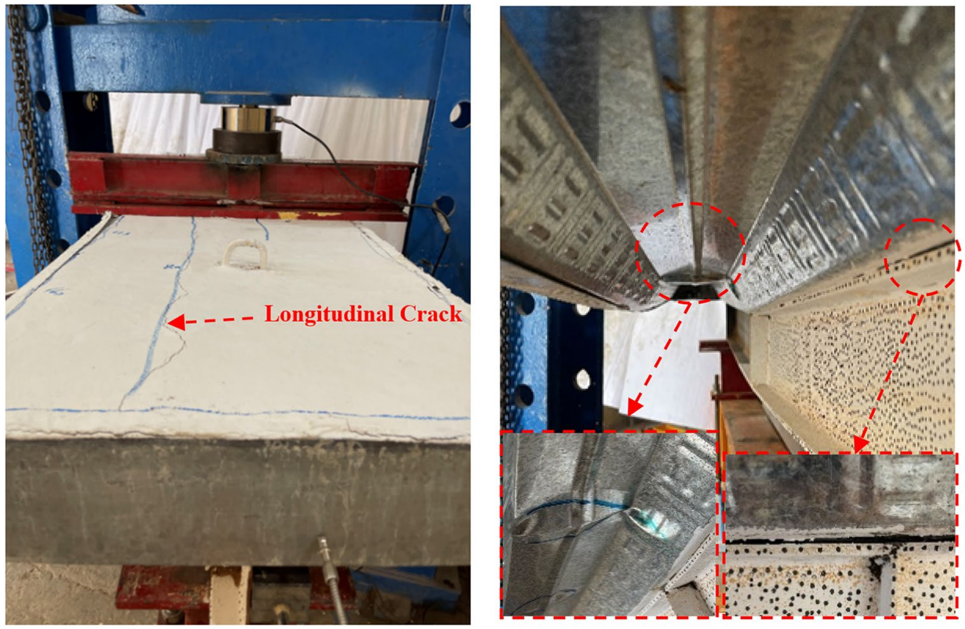

Fig. 20 Failure mode in specimen CD1

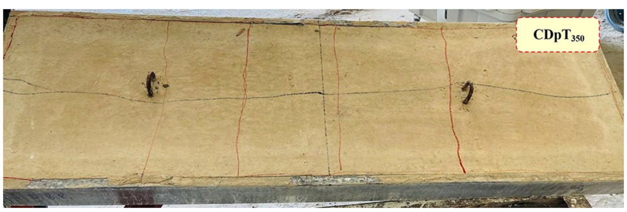

Fig. 21 Thermal and longitudinal cracking in specimen CD1T350

Fig. 22 Thermal and longitudinal cracking in specimen CD1T550

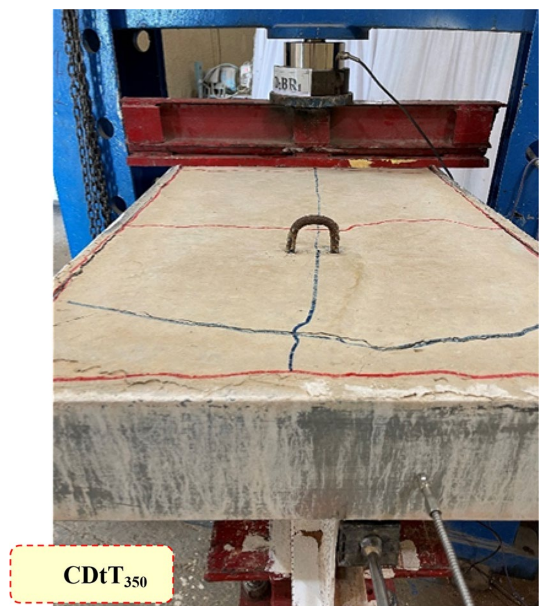

Fig. 23 Thermal and longitudinal cracking in specimen CD2T350

In a similar manner, CDt displayed similar behavior to CDp. However, the first longitudinal crack appeared at a higher load of approximately 92 kN, with a smaller width of approximately 0.1 mm. This crack initiated near the load region at 91 kN and extended continuously towards the support region.

In contrast, the failure of the burning composite beams $CDpT_{350}$ and $CDpT_{450}$ was attributed to shear connector failure, characterized by the dislocation of the shear connector from the steel beam with a brittle failure mode. Longitudinal cracks also appeared on the top face of the slab, as depicted in Fig. 21. Specimen $CDpT_{550}$ exhibited a similar behavior to $CDpT_{350}$ and $CDpT_{450}$, but with a greater number of observed longitudinal cracks on the top of the composite slab, as shown in Fig. 22.

Furthermore, a different behavior was observed for $CDtT_{350}$, where a transverse crack appeared near the support region after the appearance of the longitudinal crack, as illustrated in Fig. 23. This led to the failure of

Fig. 24 Shear connecter failure

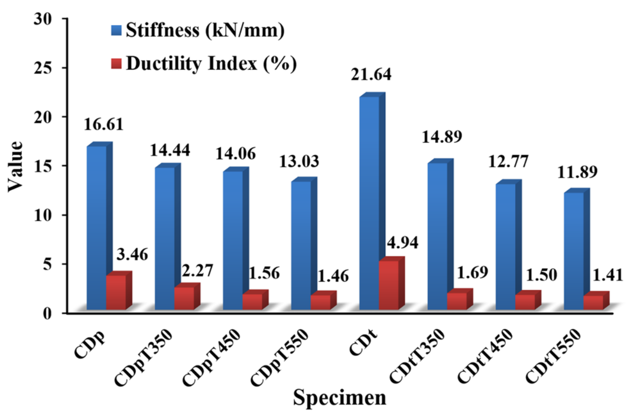

Fig. 25 Results of stiffness and ductility indices for tested specimens

the specimen through concrete and shear connector failure. On the other hand, specimens $CDtT_{450}$ and $CDtT_{550}$ failed directly as a result of shear connector failure, resulting in a brittle failure mode, as seen in Fig. 24.

4.4 Stiffness and ductility

In order to assess the effects of fire exposure on the stiffness of the composite beam specimens, the initial stiffness of the burned specimens was meticulously computed and compared with the corresponding unburned (control) specimens. The initial stiffness was determined by calculating the secant of the force versus displacement curve, specifically passing through the point where the applied force reaches 75% of the ultimate load [23]. By analyzing the initial stiffness, valuable insights into the structural integrity and performance of the specimens after fire exposure were obtained.

The results of the initial stiffness analysis are concisely summarized and graphically presented in Fig. 25, enabling a clear and comprehensive comparison between the fire-exposed specimens and their unburned specimen.

The results presented in Fig. 25 demonstrate, as expected, a decrease in initial stiffness for all the burned specimens when compared to the unburned (control) specimen. Specifically, specimens $CDpT_{350}$, $CDpT_{450}$, and $CDpT_{550}$ exhibited reductions in initial stiffness of 13%, 15%, and 22%, respectively, in comparison to the unburned specimen CDp. Moreover, specimens $CDtT_{350}$, $CDtT_{450}$, and $CDtT_{550}$ displayed even more significant decreases in initial stiffness, with reductions of 31%, 41%, and 45%, respectively, compared to the unburned specimen CDt.

This decrease in initial stiffness can be attributed to the impact of elevated temperatures on the concrete and steel components of the composite beam. The high temperatures caused the steel to experience a loss in strength and stiffness, leading to an overall reduction in the stiffness of the beam. Additionally, the high temperatures induced thermal expansion and cracking in the concrete, resulting in a deterioration of its mechanical properties. The observed decrease in initial stiffness of the burned composite beam specimens, in comparison with the unburned ones, can be attributed to the combination of weakened steel and concrete materials.

It is worth noting that the extent of stiffness reduction varied depending on the level burned specimen temperature. The differences in initial stiffness reflect the combined effects of thermal damage to steel and concrete, which resulted in reduced overall stiffness in the burned composite beam specimens.

Regarding ductility, the evaluation of ductility for the composite beam specimens involved the calculation of the ductility index, which is the ratio of the ultimate displacement (Δu) to the yielding displacement (Δy) [24]. The ultimate displacement represents the displacement recorded at the ultimate load, while the yielding displacement was determined using the method proposed by Park [25].

From Fig. 25, it is evident that an increase in the temperature of burning the specimens resulted in a greater reduction in ductility. The ductility index of the burned specimens $CDpT_{350}$, $CDpT_{450}$, and $CDpT_{550}$ was approximately 35%, 55%, and 58% lower than that of the CDp, respectively. Similarly, the reduction in ductility for specimens $CDtT_{350}$, $CDtT_{450}$, and $CDtT_{550}$ was approximately 66%, 70%, and 72% than that of the CDt, respectively.

The decrease in ductility can be attributed to the sudden failure of the burned specimens through shear connectors due to high stress concentration before reaching their full load-carrying capacity. The elevated temperatures caused

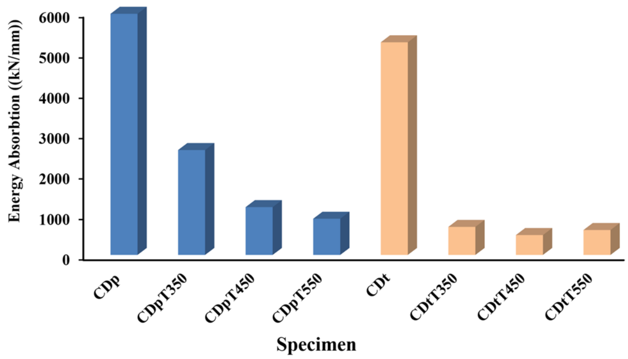

Fig. 26 The results of energy absorption capacity for all tested specimens

weakening of the steel and concrete materials, leading to reduced structural integrity and load-bearing capacity.

4.5 Energy absorption capacity

The energy absorption capacity is determined by analyzing the load–deflection curve and calculating the integral of the curve. The data presented in Fig. 26 indicates that an increase in temperature of the burned specimens leads to a decrease in the energy absorption capacity of the composite beam specimen.

Specifically, for specimens with parallel profiled sheeting (CDpT_{350}, CDpT_{450}, and CDpT_{550}), the reduction in energy absorption capacity is about 57%, 80%, and 85% than that of the specimen CDp. Similarly, for the specimens with transverse profiled sheeting (CDtT_{350}, CDtT_{450}, and CDtT_{550}), the reduction in energy absorption capacity is about 87%, 91%, and 88% than that of the specimen CDt.

At ambient temperature, the specimen with parallel profiled sheeting (CDp) has an energy absorption capacity that is about 13% higher than that of the specimen with transverse profiled sheeting (CDt). Additionally, under fire exposure conditions, all specimens with parallel profiled sheeting exhibit greater energy absorption capacity than those with transverse profiled sheeting.

5 Research impact and key findings

Fires can pose a significant threat to civil infrastructure, particularly to steel and composite beams, which can fail within 20–45 min in a severe fire incident. This leaves little time for occupants to evacuate or firefighters to control the blaze. The failure of beams can occur due to various limiting states, such as flexure, shear, or deflection. However, current codes and standards do not provide guidelines for the behavior of the new type of X-HVB shear connector in such situations. To address this gap, this paper presents the behavior of this connector in composite beam under different firing temperature.

The study's key findings reveal that the X-HVB shear connector is highly sensitive to elevated temperatures, resulting in a change from ductile to brittle behavior. Additionally, the open areas between the steel and profiled steel beam can create points of weakness in specimens with transverse profiled steel plates. To mitigate this risk, it is advisable to use suitable types of insulating materials to protect these areas in case of a fire.

6 Conclusion

This study investigates the performance of a composite beam–slab structural system utilizing the Hilti X-HVB shear connector during fire exposure. The research findings provide valuable insights into the load-carrying capacity of the composite beam under fire conditions, leading to significant conclusions:

1. The fire exposure temperature level has a significant effect on the behavior of composite steel–concrete beams. As the fire exposure temperature level increases, the ultimate load capacity and stiffness of the beams decrease. This is due to the degradation of the mechanical properties of the steel and concrete at elevated temperatures.
2. The orientation of the profiled steel deck also has a significant effect on the behavior of the beams. Beams with parallel profiled steel decks have better fire performance than beams with transverse profiled steel decks. This is because parallel profiled steel decks provide more shear resistance between the steel beam and the concrete slab, which is critical for load transfer in fire-exposed conditions.
3. At ambient temperature, the composite beam featuring transverse profiled steel demonstrates an enhanced stiffness of approximately 33% in comparison to the beam with parallel profiled steel. This variation in stiffness between the two configurations indicates the influence of the steel profile orientation on the overall structural behavior.
4. Specimens with transverse profiled plates exhibit a more ductile response under ambient temperature conditions. Conversely, specimens with parallel profiled plates demonstrate a greater ductile behavior when subjected to fire-exposed conditions. This contrasting behavior highlights the interplay between the profile orientation and thermal effects on the composite beam's performance.

5. The ultimate relative slip of the composite beam specimens decreases significantly as the temperature of the burned specimens increases. This is attributed to thermal expansion, material degradation, and a reduction in interfacial shear resistance between the steel beam and concrete slab.
6. Both at ambient temperature and under fire-exposed conditions, specimens with parallel profiled plates exhibit a higher energy absorption capacity than specimens with transverse profiled plates. This is because the parallel profiled plates provide more shear resistance, which allows the composite beam to deform more before failure and absorb more energy.

Based on conclusions which are drawn above, following recommendations for future work can be given:

1. Investigate the effects of different steel profile geometries on the performance of composite beams in fire-exposed conditions.
2. The effect of exposure to fire from top of concrete slab.
3. The effect of protected steel beam and the bottom of corrugated steel plate by intumescent coating.
4. Application of cartridge fired pins and X-HVB shear connectors with high strength steels should be further investigated for various contemporary structures, such as composite beams with cold-formed sections and composite columns.
5. Investigating the effect of high strength concrete on fire resistance of composite beam with X-HVB shear connecter type.
6. Investigating the effect of type of cooling.

Author contributions Mays A. Hamad wrote the main manuscript text and prepared all figures and tables in the manuscript. Haitham H. Muteb and Mustafa S. Salah reviewed and modified the manuscript. All authors reviewed the manuscript.

Funding No funding was received to assist with the preparation of this manuscript.

Data availability All data available in manuscript text.

Declarations

Conflict of interest On behalf of all authors, the corresponding author states that there is no conflict of interest.

References

1. Muteb HH, Hamad MA (2023) "Influence of fire in composite steel-concrete beam: review of literature." In: AIP Conference Proceedings. AIP Publishing, New York
2. Salah MS, Muteb HH, Hamad MA (2023) The structural behavior of composite cold-formed steel beam-to-column joints with different connection shapes. J Build Pathol Rehabil 8(1):50
3. Crisinel M (1990) Partial-interaction analysis of composite beams with profiled sheeting and non-welded shear connectors. J Constr Steel Res 15(1–2):65–98
4. Sanad AM, Rotter JM, Usmani AS, O'Connor MA (2000) Composite beams in large buildings under fire—numerical modelling and structural behaviour. Fire Saf J 35(3):165–188
5. Lyu J, Chen Q, Xue H, Cai Y, Lyu J, Zhou S (2020) Fire resistance of composite beams with restrained superposed slabs. Adv Mater Sci Eng. https://doi.org/10.1155/2020/7109382
6. Kodur VKR, Naser M, Pakala P, Varma A (2013) Modeling the response of composite beam–slab assemblies exposed to fire. J Constr Steel Res 80:163–173
7. Jian-chun Z, Da-shan Z, Yu-li D, Wei-hua W (2019) Experimental study on internal force variation of steel-concrete composite beam under fire. China Civ Eng J 36(6):183–192
8. Kodur VKR, Naser MZ (2018) Approach for shear capacity evaluation of fire exposed steel and composite beams. J Constr Steel Res 141:91–103
9. Ding R, Fan S, Wu M, Li Y (2021) Numerical study on fire resistance of rectangular section stainless steel-concrete composite beam. Fire Saf J 125:103436
10. Guoqiang L, Hongyu Z (2007) Experimental study on the fire resistance of steel-concrete composite beams. China Civ Eng J 40(10):19–26
11. Wang W, Jiang B, Ding F, Wang L (2023) Numerical analysis on mechanical behavior of steel-concrete composite beams under fire. Struct Des Tall Spec Build 32(10):e2012
12. Choi S (2019) Experimental studies on the behaviour of headed shear studs for composite beams in fire. Steel Compos Struct 32(6):743–752
13. Rodrigues JPC, Laím L (2014) Experimental investigation on the structural response of T, T-block and T-perfobond shear connectors at elevated temperatures. Eng Struct 75:299–314
14. Fike R, Kodur V (2011) Enhancing the fire resistance of composite floor assemblies through the use of steel fiber reinforced concrete. Eng Struct 33(10):2870–2878
15. Wang T, Hsu TTC (2001) Nonlinear finite element analysis of concrete structures using new constitutive models. Comput Struct 79(32):2781–2791
16. Nguyen XT, Park JS (2021) Inelastic strength for fire resistance of composite I-beam covered by insulation material subjected to basic loading condition. Metals (Basel) 11(5):739
17. Gluhović N, Marković Z, Spremić M, Pavlović M (2016) Experimental investigation of X-HVB shear connectors in prefabricated composite decks. Zb. Rad. građevinskih Konstr. Srb. Simp. Zlatibor. 439–448
18. Johnson RP, Anderson D (2004) Designers' guide to EN 1994-1-1: eurocode 4: design of composite steel and concrete structures. General rules and rules for buildings. Thomas Telford
19. ANSI/AISC 360-05 (2005) Specification for structural steel buildings, American Institute of Steel Construction, Chicago
20. EN1994-1-1, Eurocode 4 (2004) Design of Composite Steel and Concrete Structures. Part 1-1: General Rules and Rules for Buildings. Brussels, Belgium: European Committee for Standardization
21. HILTI Direct Fastening Technology Manual (2014) S.E. & O, Germany
22. Gluhović N, Marković Z, Spremić M, Pavlović M (2017) 08.30: Experimental investigation and specific behaviour of X-HVB shear connectors in prefabricated composite decks. ce/papers 1(2–3):2080–2089
23. Salah MS, Muteb HH (2023) The effect of cross section type on the performance of different sized bolted shear connectors

for composite cold-formed steel beams. J Build Pathol Rehabil 8(1):1–9
24. Yoo D-Y, Yoon Y-S (2015) Structural performance of ultra-high-performance concrete beams with different steel fibers. Eng Struct 102:409–423
25. Park R (1989) Evaluation of ductility of structures and structural assemblages from laboratory testing. Bull new Zeal Soc Earthq Eng 22(3):155–166